OPEN ACCESS

University of Dundee

University of Dundee

Nodal pricing

Hakam, Dzikri

Published in:
International Journal of Energy Economics and Policy

DOI:
10.32479/ijeep.6747

Publication date:
2018

Licence:
CC BY

Document Version
Publisher's PDF, also known as Version of record

Link to publication in Discovery Research Portal

Citation for published version (APA):
Hakam, D. (2018). Nodal pricing: The theory and evidence of Indonesia power system. *International Journal of Energy Economics and Policy*, *8*(6), 135-147. https://doi.org/10.32479/ijeep.6747

General rights
Copyright and moral rights for the publications made accessible in Discovery Research Portal are retained by the authors and/or other copyright owners and it is a condition of accessing publications that users recognise and abide by the legal requirements associated with these rights.

Take down policy
If you believe that this document breaches copyright please contact us providing details, and we will remove access to the work immediately and investigate your claim.

Download date: 27. Apr. 2025

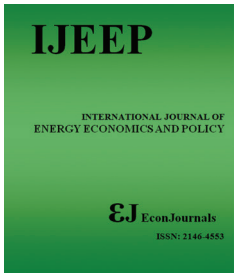

International Journal of Energy Economics and Policy

ISSN: 2146-4553

available at http: www.econjournals.com

International Journal of Energy Economics and Policy, 2018, 8(6), 135-147.

Nodal Pricing: The Theory and Evidence of Indonesia Power System

Dzikri Firmansyah Hakam[1,2]

[1]Centre for Energy, Petroleum and Mineral Law and Policy. University of Dundee, Scotland, United Kingdom, [2]PT. PLN (Persero), Jakarta, Indonesia. Email: d.f.hakam@dundee.ac.uk

Received: 11 June 2018 **Accepted:** 23 September 2018 **DOI:** https://doi.org/10.32479/ijeep.6747

ABSTRACT

This research presents a stylised nodal pricing model of Indonesia power system with engineering-economic constraints. The modelling in this research adopts the 8 nodes stylised model for the Sumatra power system, by incorporating generation, transmission and power system stability constraint. Nodal pricing analysis is performed based on direct current optimal power flow and marginal cost calculation in each node. This research is the first ever to estimate nodal prices in the Indonesian electricity market. Nodal pricing model in this paper provides a proper investment signals for Indonesian stakeholder in performing generation expansion planning.

Keywords: Nodal Pricing, Sumatra Power System, Stylised Model
JEL Classifications: C610, D410, D470, D600

1. INTRODUCTION

Nodal pricing provides an economic signal by simultaneously clearing the market by incorporating generation and demand function as inputs. The nodal pricing concept underlines the fundamental theory in determining an optimal electricity price to achieve welfare maximisation under specific constraints. Nodal market pricing reflects the opportunity costs of serving a marginal increase in demand while complying with transmission constraints. Nodal pricing provides several advantages to the market agents: Increasing market welfare, providing proper investment signals to the generator and ignoring bypass issue, i.e., the opportunity to leave the market if price is not equal to marginal cost (Green, 2007).

Schweppe et al. (1988) established the concept of nodal pricing. Nodal pricing analysis is performed based on optimal power flow (OPF) and marginal cost calculation in each node. The bidding action from the generating firm is a single shot game. The GenCos submit their fixed supply function to the ISO by acknowledging their rivals bid function. This one-shot gaming is for one bidding time interval; thus, the ISO clears the market after all the firms submit their bids resulting in the market clearing price. The market clearing price is a numeric calculation from the ISO by considering the generation and transmission network structure in the market. In other words, it is based on the electricity supply-demand balance and welfare maximisation. The ISO pays the electricity price to all generating firms in the form of a bus-nodal price based on the amount of electricity power sold to the electricity pool, while the consumer pays the electricity price to the ISO based on the active power load received.

Macatangay (1998) implemented the concept of nodal pricing in England and Wales's market incorporating transmission constraint and optimised the electricity price as a dual value in the programme. Green (2007) included transmission losses in the OPF to apply the concept of nodal pricing to the England and Wales market. In this research, the transmission loss is assumed to be relatively small and negligible. Thus, the load flow formulation is approximated by the direct current (DC) load flow equation. The

This Journal is licensed under a Creative Commons Attribution 4.0 International License

equilibrium structure in this study was applied to calculate Nash equilibrium for a particular bid function and electricity network. The power flow follows the rule of Kirchhoff's law which states that electricity injection in a particular node/bus is equal to the vector sum of the electricity input and output.

The Indonesia power system consists of two primary power systems, i.e., Sumatra and Java-Bali power system. The current academic literature on Indonesia power system is limited to the technical aspect of Sumatra and Java-Bali power systems. Optimal power flow studies the on Java-Bali power system was conducted by Wartana et al. (2012) while optimal power flow studies on the Sumatra power system was conducted by Hakam et al. (2011). Hakam and Asekomeh (2018) provides the overview of Indonesia power system while Hakam et al. (2012) provides the overview of Sumatra power system and energy mix. Faizal et al. (2015) conducted the power system studies on the future interconnection of Sumatra-Java system through a HVDC transmission system. The majority of existing research discussed the technical aspect of the grid, i.e. load flow analysis, short circuit, and stability analysis. For example, Hakam et al. (2011) conducted a load flow, short circuit and transient analysis of power system interconnection between the North System and Middle-South System on Sumatra's 275 kV transmission system. Although current studies are limited in the engineering aspect, these studies contributed to the scientific modelling of this research. For example, optimal load flow studies provided an insight of the upper and lower boundaries of transmission constraint according to the load flow and transient stability analysis.

The objective in this research is to develop a stylised modelling of nodal pricing in Indonesia power system. This research will simulate nodal markets under perfect competition for two power system: (1) Four node power system (2) Sumatra power system. This research is the first ever to estimate nodal prices in the Indonesian electricity market. This nodal pricing approach in Indonesia power system contributes to the current body of literature on electricity market modelling and market pricing study. The economic model developed in this research is a pioneer one based on network subsystem boundaries set up by the PLN TSOs. This research adopts the 8 nodes stylised model for the Sumatra power system, by incorporating generation, transmission and power system stability constraint. The stylised model in this research does not exactly represent the complexity of the Indonesia power system. However, it attempts to capture the important aspects of the techno-economic of Indonesia power system. Thus, stylised modelling, including electricity demand and power generation allocation for each node, is a crucial one and should incorporate all the demands and suppliers in the system.

This paper is structured into 5 chapters as follows. Chapter one, of which this section is a part, presents the introduction and overview of this research. Chapter two contains the methodology that explains the DC power flow, optimisation formula, and demand-supply function. Chapter two also applies the concept of nodal pricing in a four-node power system. Chapter three is the stylised model of Sumatra power system. Chapter four applies the nodal pricing approach in Sumatra power system. Chapter five is the conclusion.

2. METHODOLOGY

2.1. DC Power and Law of Parallel Circuit

Assuming a power setting with m transmission lines and n nodes, X is a vector of reactance ($m \times m$). P_F is a vector of DC power flow ($m \times 1$). M is the node-branch incidence matrix for an angle phase vector matrix (n-1 $\times$ m) excluding the reference node (slack bus), i.e. a node with phase angle is zero. P is the power injection matrix (n-1 $\times$ 1). B is the susceptance matrix. Based on a DC power flow assumption, the power injection in node n is the difference between power generation production q_{Si} and consumer demand q_{di}. Thus, the power flow in the transmission line could be denoted as a linear function between PTDF and q_{si}-q_{di}.

$$P_F = \sum_i PTDF(q_{si} - q_{di}) \quad \text{DC load flow as a function of PTDF} \quad (1)$$

Any form of network aggregates changes the cable limit and reactance. Thus, a transmission line alteration from double or single phi to a single circuit will influence the loop flow of the power system. Following the law of parallel circuit as in Hagspiel et al. (2014) and Hogan et al. (2010), doubling the transmission capacity will halve the line's reactance.

$$X_{ij}^n = \frac{T_{ij}^0}{T_{ij}^n} X_{ij}^0 \quad \text{The law of parallel circuit} \quad (2)$$

T_{ij}^0 is the cable limit at initial state which connects node i to j; while X_{ij}^0 is the cable reactance at initial state.

2.2. Optimisation Problem and Karush-Kuhn-Tucker Condition

Figure 1 shows the optimisation problem structure. An optimisation problem in mathematical programming is a mathematical function that has a purpose of maximising or minimising objective function subject to objective constraints (equalities and inequalities). In the case of locational marginal pricing (LMP), the objective constraints usually consist of generation capacity and cable thermal limit inequalities constraints.

Figure 1: Optimisation problem structure

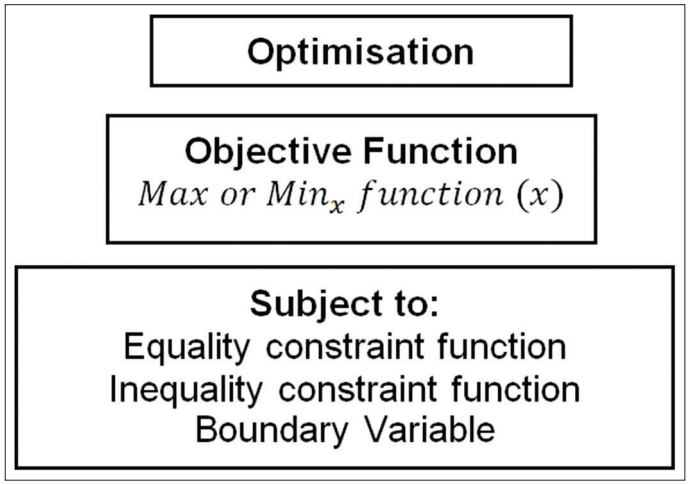

Assuming that $x \in R^n$ is the variable vector of optimisation, $f(x)$: $R^n \rightarrow R$ is the objective function, $g(x)$: $R^n \rightarrow R^e$ is the equality constraint function, $h(x)$: $R^n \rightarrow R^i$ is the inequality constraint function. The solution $x \in R^n$ is feasible if meeting the equality, inequality and bound constraints. The optimal solution occurs only if the feasible regions are meeting the objective function. The optimisation problem has a general form as follows: *Max* or $Min_x f(x)$ subject to: $g(x)=0$; $h(x) \leq 0$.

The optimisation technique in an equilibrium problem is developed as a vital tool to model and solve energy market problems under uncertainty conditions.

The principal use of KTT condition is to find a unique price and profit equilibrium in the market. The unique equilibrium result implies a convex feasible region for the generator, ISO and consumer's problem which suggest that the local optimum of the problem is also the global optimum. Thus, it is important to have a convex problem since non-convex equations will result in non-existence or multi-equilibrium. In the electricity market, the convex problem combines all market participants (supplier, transporter, and consumer) through KTT combination; thus, the equation is solved in the market clearing mechanism.

Assuming $F(x)$ is smooth and concave, and $H(x)$ is convex, the objective function is as follows:

$Max_x\ F(x)$

Subject to: $(x) \leq 0$; $x \geq 0$

Assume λ is Lagrange multiplier for H constraint, general *FOC KTT* conditions for a constrained optimisation problem above is:

$$0 \leq x \perp \frac{\partial F}{\partial x} - \lambda \frac{\partial H}{\partial x} \leq 0$$

$0 \leq \lambda \perp H \leq 0$

2.3. Supply-demand Function and Consumer-producer Surplus

The GenCos produce electricity energy based on the true generator cost while the consumer provides the demand functions which reflects the energy used. The inverse demand function is a linear function with negative slope as follows:

$p_i(q_{di}) = a_i - b_i q_{di};\ i=1,\ldots,I$	Inverse linear demand	3

Where a_i and b_i are the load demand coefficient and q_{di} is the active load demand at node i. $a_i > 0$ and I is the number of the consumer.

Total generation cost consists of fixed (f_i) and variable costs $C_i(q_{si})$:

$C_i(q_{si}) = f_i + c_i q_{si} + \frac{1}{2} d_i q_{si}^2;\ i=1,\ldots,I$	Total cost function	4
$C_i(q_{si}) = c_i q_{si} + \frac{1}{2} d_i q_{si}^2;\ i=1,\ldots,I$	Variable cost function	5

Generating firm bid/marginal cost function $MC_i(q_{si})$ is a linear function since the application of constant marginal cost is not fully representative of the true generation cost in the electricity industry. Marginal cost function is the derivative of the total cost function as follow:

$MC_i(q_{si}) = c_i + d_i q_{si};\ i=1,\ldots,I$	Marginal cost function	6

We define consumer surplus as the net consumer benefit. Thus, the total consumer surplus is the sum of each consumer surplus based on a particular price. The consumer surplus for each region could differ depending on the electricity network structure, e.g. transmission constraint, generator and consumer configuration/location. Assuming $D_i(p_i)$ is the electricity demand for consumer i at price (p_i), the consumer surplus for inverse linear demand function is:

$CS_i(p_i) = \frac{1}{2}(a_i - p_i) D_i(p_i);\ i=1,\ldots,I$	Consumer surplus	7

Producer surplus is the generator net benefit received from selling electricity demand to the power pool, defined as $PS_i(p_i)$:

$PS_i(p_i) = \frac{1}{2}(p_i - c_i) q_{si}(p_i);\ i=1,\ldots,I$	Producer surplus	8

To calculate the inverse linear demand function, it was assumed here that the reference point for q_{di} is the peak load demand in node q_0. This study categorised the LSE according to the distinction of residential and non-residential (business and industrial) node. Price data from the Indonesia Energy Ministry provides the price reference p_o.

Based on the linear inverse demand function in Equation 3, the demand function is provided as follows:

$q_{di} = \frac{a_i}{b_i} - \frac{p_i(q_{di})}{b_i};\ i=1,\ldots,I$	Linear demand function	9

The demand intercept $a_i > 0$ and slope $b_i > 0$, the elasticity of demand is calculated as follows:

$\varepsilon = \frac{\partial q_{di}}{\partial p_i(q_{di})} \frac{p_i(q_{di})}{q_{di}} = -\frac{1}{b_i} \frac{p_i(q_{di})}{q_{di}}$	Elasticity of demand	10
$b_i = -\frac{1}{\varepsilon} \frac{p_0}{q_0};\ a_i = p_0 - b_i q_0$	Calculating linear demand function from p_0 and q_0	11

Using b_i and a_i parameters, the inverse demand function for each node is calculated by assuming elasticity exogenously. The demand calculation using this approach is implemented in European nodal pricing as in Leuthold et al. (2012) and provides flexibility to conduct an analysis using various elasticity assumptions as in Green (2007).

2.4. Welfare Maximisation by ISO: Perfect Competition

The system operator manages the balancing mechanism of electricity supply from generating firms and the power demand from consumers. The ISO maximise the total welfare $\pi_i(p)$ by choosing a single price for each bus i (1,…,I) in the mesh network by taking into account network (generation and transmission) limits as inequality and equality constraints. Assuming that $P_i(q_{di})$ is the energy consumption benefit; $MC_i(q_{si})$ is the total cost of generators at node i; q_{si} is the active load supply from generator at bus i and $\overline{q}_{si}$ is the available capacity of generator at node i, the ISO welfare maximisation problem is formulated as follows:

$\max_{q_{di}} \left(\sum_i P_i(q_{di}) q_{di} - \sum_i MC_i(q_{si}) \right)$	Welfare maximisation	12
Subject to/constraints:		
$\sum_i q_{si} - \sum_i q_{di} = 0$	Electricity demand balance	13
$\sum_l PTDF\left(q_{si} - q_{di}\right) \le T_l$	Transmission constraint	14
$q_{si} \le \overline{q}_{si}$	Generation constraint	15
qdi>0 qsi>0	Non negativity	16

Definition: Assume that λ, μ_+, μ_- is Lagrange multipliers/dual variables for electricity demand balance and transmission constraint, respectively. λ is the mesh network price for all of the nodes in the power system.

Proposition 1: In a congested transmission line, the nodal prices are not uniform due to nodal prices discrimination and creating LMP.

Proof: For the ISO welfare maximisation problem, a general FOC KTT conditions for ISO mixed complementarily problem (MCP) can be derived as follows:

$P_i(q_{di}) - \lambda - \sum_l PTDF\left(-\mu_+ + \mu_-\right) = 0$ $\sum_i q_{si} - \sum_i q_{di} = 0$ $0 \le \mu_+ \perp \sum_l PTDF\left(q_{si} - q_{di}\right) - T_l \ge 0$ $0 \le \mu_- \perp -\sum_l PTDF\left(q_{si} - q_{di}\right) + T_l \ge 0$	FOC for ISO condition	17

The first *FOC KTT* condition for *MCP* above yields a general locational pricing equation:

$P_i(q_{di}) = \lambda + \sum_l PTDF\left(-\mu_+ + \mu_-\right)$	General LMP function	18

Assume $\sum_l PTDF\left(-\mu_+ + \mu_-\right) = \gamma^i$ a premium charge for transmission congestion existed in the network and formulated as the difference between nodal price $P_i(q_{di})$ and system price λ. A transmission congestion charge depends on the availability of congestion and transmission dual variables μ_+, μ_-. A firm receives payment γ^i when the firm injecting power to bus i and pays a withdrawal charge γ^j when withdrawing power at bus j, and the difference of this transmission cost is defined as a wheeling charge γ^i-γ^j. Considering the slackness condition of μ_+ and μ_+ when the transmission line is uncongested μ_+=μ_+=0, the nodal price $P_i(q_{di})$ is equal to λ and the entire nodal price will be uniform. When the transmission line is congested, $\mu_+ \ge 0$; $\mu_+ \le 0$, the bus prices are not uniform and depends on the transmission line l. (■)

In the case where there is no transmission constraint, the nodal price is equivalent for each bus. If there are any transmission constraints and congestion in the mesh network, then the ISO will calculate the market clearing price for each node based on the welfare maximisation. The generation firm could bid a supply function other than their true marginal cost function. Thus, the effect of the market price could differ depending on the generation configuration.

Definition: Load payment $\sum_i P_i(q_{di}) q_{di}$ is the net consumption payoff from the consumer at the nodal price while generation charge $\sum_i P_i(q_{di}) q_{si}$ is the energy production paid to the generator at the nodal price.

Proposition 2: The difference between load payment and generation charge is the total congestion rent η.

Proof: We calculate the difference between generation charge and load payment as follows:

$\eta = \sum_i P_i(q_{di}) q_{di} - \sum_i P_i(q_{di}) q_{si}$ $\eta = \sum_i P_i(q_{di}) [q_{di} - q_{si}]$	Congestion rent	19

Observe that $\sum_i P_i(q_{di}) q_{di}$ and $\sum_i P_i(q_{di}) q_{si}$ satisfies the KTT condition. Thus, η is calculated as follows:

$$\sum_i P_i(q_{di})[q_{di} - q_{si}] - \sum_i \left[\begin{array}{l} \lambda[q_{di} - q_{si}] - \\ [q_{di} - q_{si}] \sum_l PTDF\left(-\mu_+ + \mu_-\right) \end{array} \right] = 0$$

$$\eta = \sum_i \left[\lambda[q_{di} - q_{si}] + [q_{di} - q_{si}] \sum_l PTDF\left(-\mu_+ + \mu_-\right) \right]$$

$$\eta = \sum_i \lambda[q_{di} - q_{si}] + \sum_i \left[[q_{di} - q_{si}] \sum_l PTDF\left(-\mu_+ + \mu_-\right) \right]$$

Notice that for the KTT condition, $\sum_i \lambda[q_{di} - q_{si}] = 0$, and $\sum_l PTDF\left(-\mu_+ + \mu_-\right) = \gamma^i$ is a premium charge for transmission congestion; thus the congestion rent is premium charge times the import/export of electricity in node i $[q_{di}$-$q_{si}]$.(■)

$$\eta = \sum_i \left[[q_{di} - q_{si}] \gamma^i \right]$$

Definition: If $\sum_l PTDF\left(q_{si}-q_{di}\right)\geq T_l$ where the transmission constraint is binding to the linear function, then the transmission line l is congested; and vice versa. If $\sum_l PTDF\left(q_{si}-q_{di}\right)\leq T_l$, then the transmission line l is uncongested.

Proposition 3: In the case where transmission congestions occur in the power system, the ISO collects the surplus transmission rent.

Proof: Notice the KTT condition for transmission constraint:

$$\sum_i P_i\left(q_{di}\right)\left[q_{di}-q_{si}\right]-T_l\sum_l PTDF\left(-\mu_+ +\mu_-\right)=0$$

$$\eta=T_l\sum_l PTDF\left(-\mu_+ +\mu_-\right)$$

Since the slackness condition implies $T_l\geq 0$; $\mu_+ \geq 0$; $\mu_-\geq 0$ the congestion rent $\eta\geq 0$. The congestion premium of the transmission line being non-negative indicates that the load payment is higher than the generation charge, i.e. the dual variables are binding to the inequality condition (■).

Definition: For linear demand and marginal cost, consumer surplus and producer profit is calculated as $CS_i\left(p_i\right)=\frac{1}{2}\left(a_i-p_i\right)D_i\left(p_i\right)$ and $PS_i\left(p_i\right)=\frac{1}{2}\left(p_i-c_i\right)q_{si}\left(p_i\right)$, respectively.

Proposition 4: The congestion in transmission line results in rent transfer from consumers and producers to the ISO.

Proof: We calculate the total welfare as follows:

$TW=CS_i\left(p_i\right)+P_{Si}\left(p_i\right)$		
$TW=\frac{1}{2}\left(a_i-p_i\right)D_i\left(p_i\right)+\frac{1}{2}\left(p_i-c_i\right)q_{si}\left(p_i\right)$	Total welfare function in LMP	20
$TW=\frac{1}{2}\left(a_iD_i\left(p_i\right)-c_iq_{si}\left(p_i\right)-\left(p_iD_i\left(p_i\right)-p_iq_{si}\right)\right)$		

Notice that for transmission uncongested $a_iD_i\left(p_i\right)$-$c_iq_{si}\left(p_i\right)$=0, and for transmission congested $a_iD_i\left(p_i\right)$-$c_iq_{si}\left(p_i\right)$=0. Acknowledging proposition 2 and 3, if the transmission is congested, then the net market (producers and consumers) surplus is below the total market welfare. The ISO captures the difference of this welfare (■).

2.5. Small Scale Nodal Pricing

In a real power system topology, the power system consists of multiple sub-networks with each node consisting of one LSE and single or multi power plant technologies. Each power plant has a distinctive linear marginal cost which represents unique generation technology, e.g. base, intermediate and peaking PP. The generation technology mix of a power system could be divided based on the ability of the PP to ramp-up and ramp-down to adjust the electricity demand fluctuation from LSE aggregate. Ramping rate, low fuel cost and long construction time are characteristics of baseload power plant. In contrast, high ramping rate, high fuel cost, and relatively low construction time are characteristics of peak load power plant. A four-node electricity network is used here to determine the technical and economic insights of nodal pricing in power system. Four-node market configuration.

Figure 2 presents the configuration of the interconnected four-node system. Assume a four-node interconnected power system with each node consisting of one power plant and one LSE. The four transmission lines are identical. Thus, they have similar admittance and resistance for each subsection. The simulations were conducted in two transmission conditions which are congested and uncongested transmission lines. For the transmission-constrained condition, line 2–3 and line 1–4 are limited to 2 MW, which defines that power flow from node 2 to node 3 and from node 3 to node 2 is limited to 2 MW. The transmission line characteristics (resistance and admittance) and AC flow variable (phase and voltage angle) influence the congestion nominal. Table 1 shows the shift factor matrix for four-node power system with uniform lines. Since DC load flow is applied, this simulation considers PTDF as a function of shift power factor and power injection. Node no. 4 is chosen as a slack bus and assuming a zero-reference angle for this node by deleting the row and column of slack bus impedance matrix. DC load flow calculation uses transmission line's shift factor matrix. The solution for shift factor matrix is as follows:

Table 2 provides the linear demand function for each LSE, and supply function from each power plant. Exogenous electricity demand consists of residential and industry demand. Hence, these electricity demands aggregated in power substation as a linear price function. The LSE for each node applies inelastic demand. Generation capacity constrains power plant output. The biggest supplier of the system is GenCo3 with a capacity of 120 MW while the smallest player is GenCo 1 with a capacity of 30 MW. The variety of marginal cost function in this model represents the mix of generation technologies in the real power system.

Figure 2: Four nodes interconnected power system

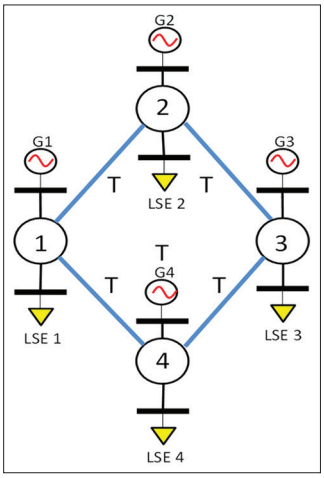

Table 1: Shift factor matrix for four-node power system with uniform lines

0.25	−0.5	−0.25
0.75	0.5	0.25
0.25	0.5	−0.25
0.25	0.5	0.75

Figure 3: Case 1. Unconstrained transmission power system

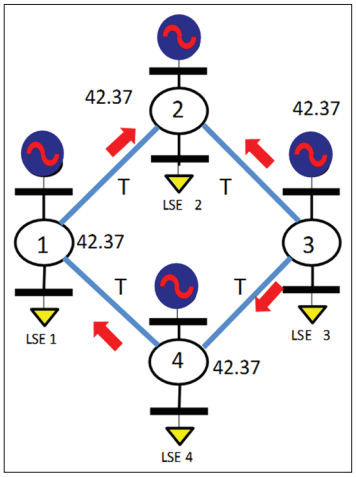

Figure 4: Case 2. Constrained transmission power system

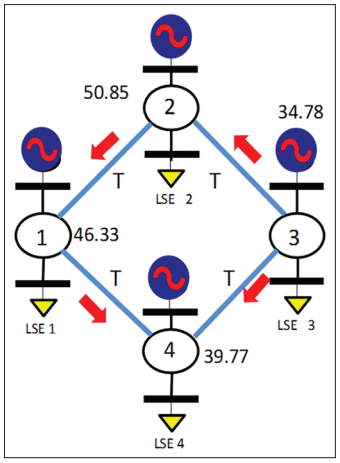

The market simulation was conducted by calculating two different case studies. The first case study is unconstrained transmission while the second case study is constrained transmission. Load flow and price-quantity equilibrium from this power system modelling is obtained as can be seen in Tables 3 and 4.

The first case study as in Figure 3 is an unconstrained network in a perfect competition environment. As shown in Table 3, the equilibrium price is uniform across the regions with a nominal 42.37 $/MWH. The uniform price occurs due to the uncongested transmission lines. The electricity could flow to any LSE based on the economic signals provided from real marginal cost and demand. Node one and four were utilising all of its generation since GenCo 1 has the lowest marginal cost and GenCo 4 has a relatively small marginal cost compared to GenCo 2 and 3. The load flow result (Table 4) follows the Kirchoff law. Node 1 is a deficit region where GenCo 1 with a capacity of 30 MW supplies a 37.63 MW electricity demand. The load-flow mechanism (PTDF) balances this energy shortage by importing 9.13 MW of electricity from node 4 and exporting 1.5 MW of power to node 2. Please note that the arc and nominal of power flow is according to the Kirchhoff law, i.e., the sum of energy flow for all nodes is equal to zero. By calculating the supply bidding from each supplier and the consumers demand from LSE's, the system operator clears

Table 2: Maximum capacity, demand and marginal cost

n	k_i (MW)	a_i	b_i	c_i	d_i
1	30	80	1	20	0.2
2	70	100	0.8	25	0.4
3	120	90	1	15	0.3
4	40	85	0.9	20	0.3

Table 3: Output q_{si} (MW), demand q_{di} (MW) and price ($/MWH)

n	Case 1			Case 2		
	q_{si}	q_{di}	p_i	q_{si}	q_{di}	p_i
1	30	37.63	42.37	30	34	46.33
2	43.43	72.04	42.37	65	61	50.85
3	91.24	47.63	42.37	66	55	34.78
4	40	47.37	42.37	40	50.25	39.77

Table 4: DC load flow (MW)

From *i*	to *j*	P_{ij} (DC) case 1	P_{ij} (DC) case 2
1	2	1.50	(5.19)
1	4	(9.13)	1.53
2	3	(27.11)	(2.00)
3	4	16.49	8.72

the market price to set quantity equilibrium. Similar to case 1, the shadow prices - occurring at node 1 and 4 - are bounded by the generation constraint, although at a higher level due to the additional congestion from the cable limits. Demand and supply equilibrium Q in the interconnected power system is converging at level 204.66 MW.

Transmission congestion affects the market equilibrium since the cable limit bounded the import and export of the electricity. As can be seen in Figure 4, the price in each node is varied. The highest price in the system is 50.8 $/MWH located at node 2 reflecting the high production cost in region 2. The initial power flow from node 1 to node 4 is limited to 2 MW from 9.13 MW, previously, which results in 1.53 MW load flow. The transmission line that is connecting node 2 and 3 is applying the similar nominal constraint, which affects the load flow causing it to reduce from 27.11 MW to 2 MW.

3. THE MODEL

Sumatra and Java-Bali power system are two of the largest power system in Indonesia. The simulation setup in this research is limited to Sumatra power system. The simulation was performed using perfect competition with normal operation based on PLN power flow data for the year 2015 to derive the economic signals. Each node was modelled as an individual player who represents one GenCo. Note that in the Sumatra system, one GenCo only serves one LSE/subsystem. All of the power system data was collected from PLN according to the references in PLN (2015), (P3BS 2016a), and (P3BS 2016b). These power system data are accessible as publicly available datasets. PLN published these reports for power system planning, evaluation, and investment purposes. The list of data collections are as follows:

1. Demand: Non-coincident peak load for the Sumatra system.
2. Generation: Maximum and available capacity,[1] generation

1 Available capacity is the power plant capacity based on the availability

technology and fuel type and fuel cost. The linear marginal cost data was calibrated according to the realisation of generation cost and output from each power plant.

3. Transmission configuration and characteristic. We collect reactance and transfer limit to perform DC load flow analysis. This research applies a stylised model based on the actual network configuration of the 150 kV Sumatra system. To acquire a precisely stylised model, the model was cross-checked with the PLN TSOs.[2] The reactance data is for a single circuit. Thus, the reactance rating for parallel cable follows the law of parallel-circuit.
4. Load flow realisation. PLN TSOs conduct load flow analysis using power system software, e.g. Digsilent and PSSE. PLN provides the Sumatra power system planning in P3BS (2016b). The base case scenario was adjusted for constrained nodal pricing based on power flow realisation from P3BS (2016a).

The power plant available capacity includes the generation from PLN, IPP and other power plant, i.e., rental PP and excess power (e.g. excess power from the Aluminum Plant in South Sumatra). The linear demand function was calculated according to the actual peak load for each node, assuming that the price elasticity of demand is inelastic for all areas. The generation cost was derived using power plant data, e.g. fuel cost, fuel consumption rate and efficiency. The intercepts and slopes of marginal cost were calibrated, assuming linear marginal cost curves, according to the generation transaction cost of PLN in 2015. The intercept and slopes of the demand curves were calibrated, assuming elasticity reference 0.15 and price reference 97.98 $/MWH, according to the approach by Leuthold et al. (2012).

The price reference is based on Ministry of Energy and Mineral Resources Regulation No. 31 2014 regarding electric energy tariffs provided by PLN (Assuming 1$ = 13,799 IDR in 2015). The electricity tariff in Indonesia is varied according to the type of usage, i.e., residential, business, industry, and social. The electricity tariff also varied according to the circuit breaker capacity. For example, in residential tariff, R-1/TR (up to 450 VA) has a tariff of 415 IDR/KWH, R-2/TR (up to 900 VA) has a tariff of 605 IRD/KWH, while R-1/TR (up to 1300 VA), R-2/TR (up to 2200 VA), R-3/TR (3500–5500 VA), and R-4/TR (above 6600 VA) have a tariff of 1352 IDR/KWH (equal to 97.98 $/MWH). The electricity tariff of 97.98 $/MWH is also charged for the highest type of business consumer, i.e. above 6600 VA. Thus, this electricity tariff was chosen as a price reference in our modelling since the electricity tariff for R-1/TR (up to 450 VA) and R-2/TR (up to 900 VA) is subsidised by the Indonesian government. The electricity tariffs for industry and social customer are also below 97.98 $/MWH since the electricity tariff for both customers are incentivised and subsidised, respectively. For full Indonesia electricity tariffs, see ESDM (2015).

The generation data characteristics presented are the available capacity of a node , power plant allocation and marginal cost for each node. Short run marginal cost is constructed by taking into account fuel cost, heat rate and energy production, and the availability factor (AF) of each unit plant. These data are available from the 2015 operational realisation data of P3BS. The generation capacity of each GenCo is bounded not by maximum capacity k_i but by available capacity $\overline{q}_{si}$ and outages at particular period $k_i = AFx\overline{q}_{si}$ where AF is the AF which accommodates the machine de-rating of the power plant. For power plants that operate in 2015, the AF also takes COD time into the calculation, i.e. the actual time when the power plant energies and supplies electricity to LSEs. Note that this model assumes that hydropower plant operates at maximum capacity as in the wet season.

The stylised model in this research is acquired by transforming the original network configuration as in Figures 5-8 by applying the law of parallel circuit. The electricity market modelling in this research applies the law of parallel circuit to acquire accurate load flow analysis. Figure 5 shows the single line diagram of the 150 kV North Sumatra subsystem. As shown in the Figure 5, the North Sumatra subsystem is already connected by a 275-kV subsystem through the connection of a transformer connecting the Binjai 150 kV to the Binjai 275 kV substation. The power generation mix in north Sumatra is comprised of coal, gas, hydro, and diesel PP. Figure 6 shows the single line diagram of the 150 kV mid-Sumatra subsystem. The Mid Sumatra subsystem connects the North Sumatra with the South Sumatra subsystem. Further, the Mid Sumatra subsystem is abundant with hydro energy sources which has resulted in lower fuel costs compared to the North and South subsystems. The South Sumatra subsystem is illustrated in Figures 7 and 8, and consists of a 150 kV and 70 kV transmission network.

The power system modelling in this research defined the market boundaries of Sumatra power system based on P3BS (2016a). One bus in the Sumatra model represents one player in the network. The simulation was performed based on non-coincident peak load data for 2015. The served peak load on the North Sumatra power system is 1839 MW, take place at Thursday, on the 3rd September 2015 at time 19.30, while the served peak load in the Mid-South Sumatra subsystem is 3,048 MW, held at Tuesday, on the 18 August 2015 at time 19.00.

Figure 9 shows the stylised network of the Sumatra power system while Figure 10 shows the Sumatra power system map. The Sumatra power system is divided into eight nodes according to PLN subsystem division; each node contains one GenCo and one LSE. The South Sumatra subsystem consist of two nodes, i.e. Aceh and Sumut; the Mid Sumatra subsystem consists of two nodes, i.e. Riau and Sumbar; the South Sumatra subsystem is divided into the Jambi, Sumsel, Bengkulu and Lampung nodes. The load and generation allocation for the Sumatra power system is shown in Table 5.

Table 6 shows the transmission characteristics for the Sumatra power system, e.g., node connections, type of configurations, base reactance and thermal limit. Note that the type of transmission configuration affects the reactance nominal. Hence, transmission aggregation is performed to transform the granular power system into a stylised model. The cable limits for a parallel transmission line is equal with the limits of the basic network. The reactance

factor that represents the actual generation capability of a power plant installation. Availability factor takes account of the real curtailment/outages at a particular power plant.

2 Each power system has its own TSO, Sumatra's TSO (P3BS) is responsible for the power system operation and transmission assets in the Sumatra.

Figure 5: Single line diagram of 150 kV north Sumatra subsystem 2015 (P3BS 2016b)

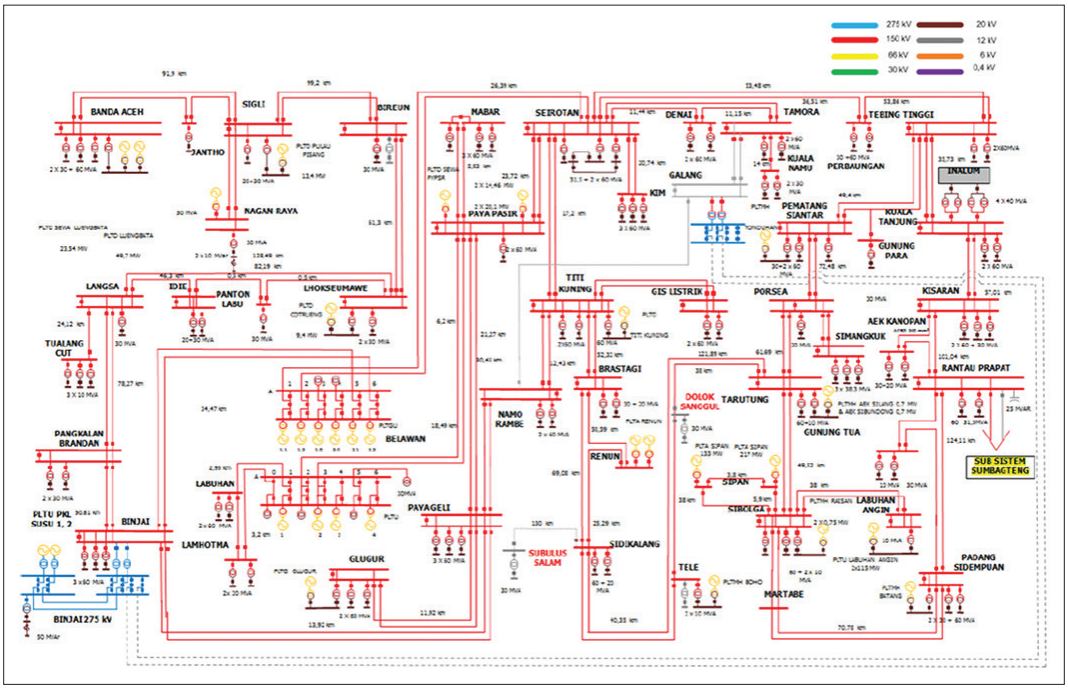

Figure 6: Single line diagram of 150 kV mid Sumatra subsystem 2015 (P3BS 2016b)

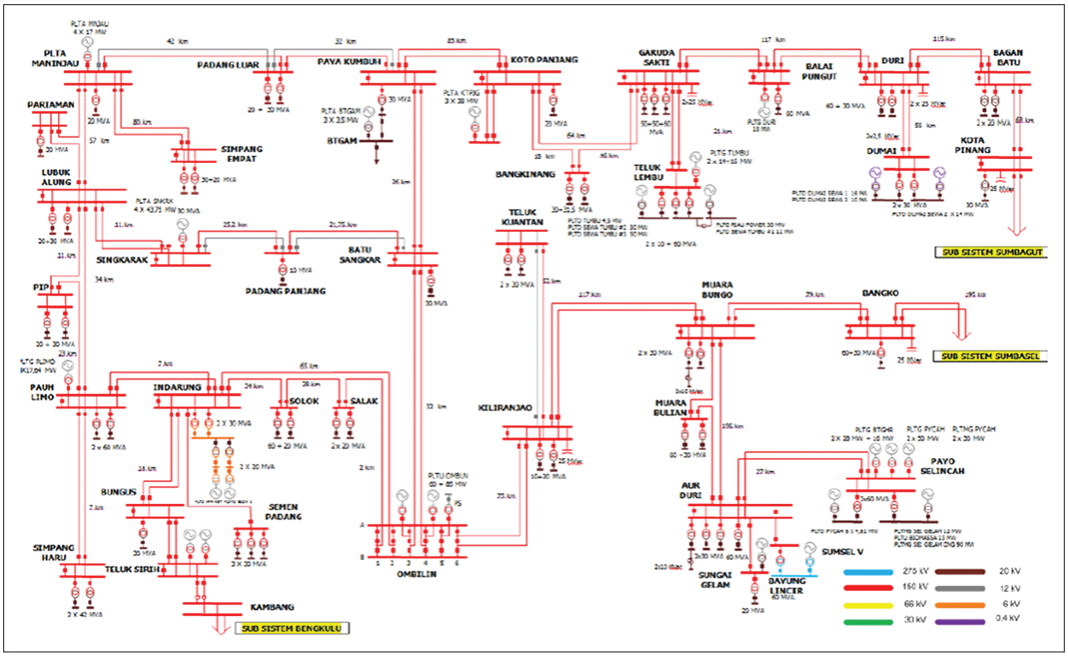

of transmission line connecting node i to j (X_{ij}) is in per unit, calculated by dividing each reactance nominal to the highest reactance in the particular power system.

4. RESULT

Table 7 shows the shift factor matrix for the Sumatra power system. Subsystems in the Sumatra power system are connected by a radial transmission configuration. Thus, the calculation of Sumatra's load transfer distribution factor is trivial to solve compared to a loop configuration.

Table 8 shows the nodal demand, generation and welfare for Sumatra nodal pricing. The Sumatra power system is not a regional balance system since some of the subsystems need energy import from another subsystem to meet local energy demand. Aceh, Riau, and Lampung are the deficit regions according to their energy insufficiency to meet subsystem demand. Note that being a surplus region does not automatically define the region as an energy exporter. Aceh and Jambi produced zero energy production since Aceh produce a higher electricity price compared to Sumut, while Jambi produces a higher electricity price compared to South Sumatra. The total demand is equal to the total supply (5,101.8 MW).

Figure 7: Single line diagram of 150 kV south Sumatra subsystem 2015 (P3BS 2016b)

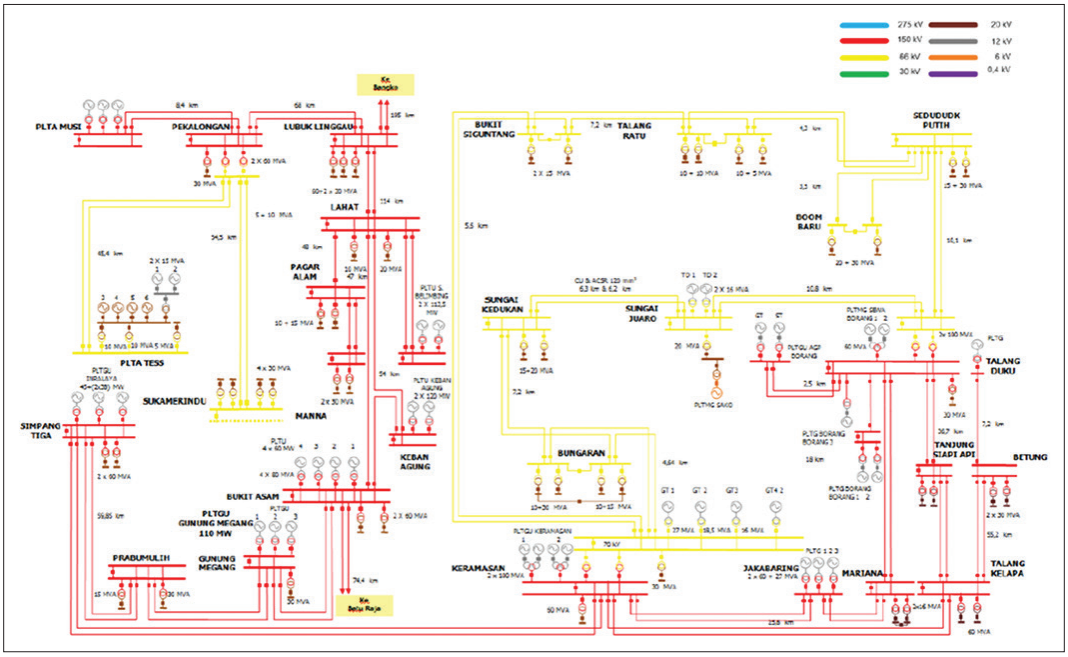

Figure 8: Single line diagram of 150 kV south Sumatra subsystem (P3BS, 2016b)

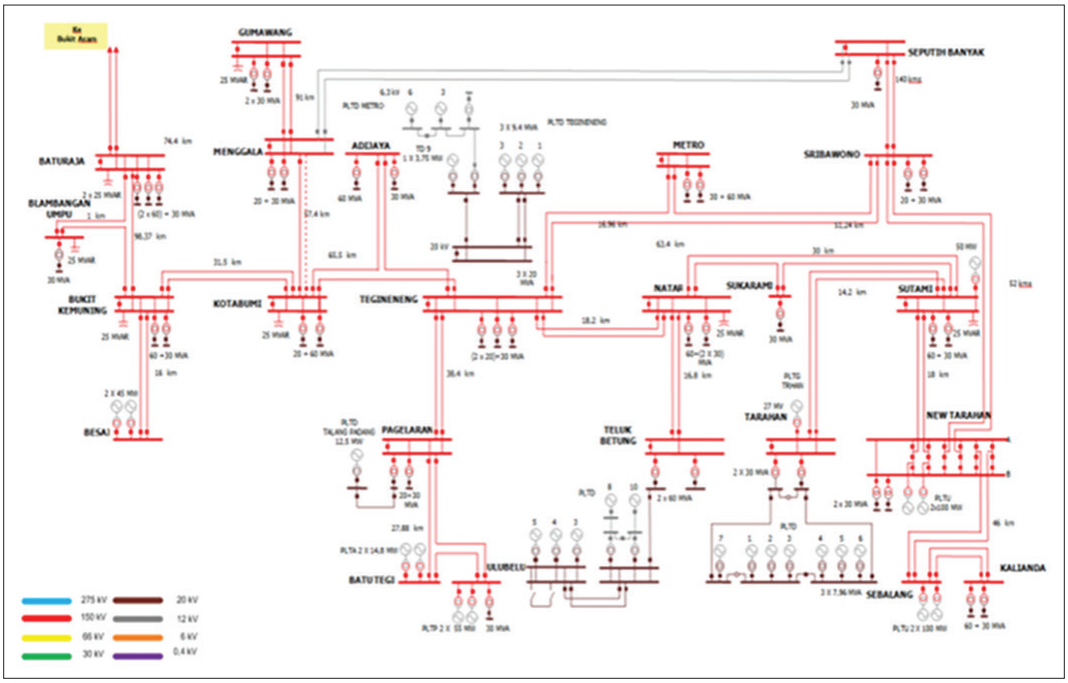

The Sumbar and Bengkulu subsystems are dominated by hydro PP with low fuel cost. Thus, these two subsystems produce cheaper generator capacity to meet local and connected subsystem demands.

Power system constraints consist of transmission constraint that reflects the flow of active power and voltage constraints which determined the amount of reactive power flow. In the Sumatra model, the voltage constraints were transformed into thermal limits to make the modelling more reliable. Thus, the application of the DC model in this research does not underestimate the voltage constraints caused by reactive power transfer. The Sumatra power

Figure 9: Stylised network of Sumatra power system

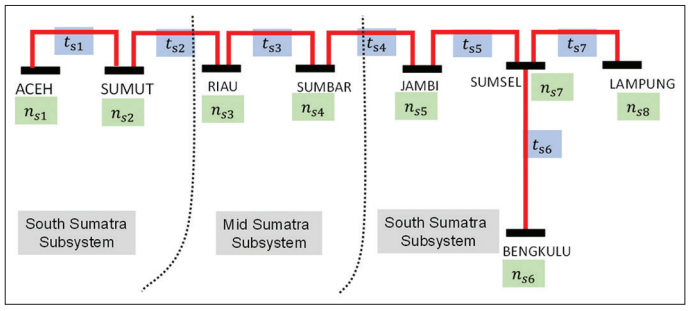

Table 5: Load and generation allocation for Sumatra power system

Node	Subsystem	q_{di} (MW)	$\overline{q}_{si}$ (MW)	Power plant	(MW)	mc ($/MWH)
n_{s1}	Aceh	290	264.2	Nagan Raya	160	85.83
				KKA Lhokseumawe	20	
				Lueng Bata	31.9	
				Cot Trueng	12.5	
				Pulau Pisang	9.8	
				Sewa Aggreko	30	
n_{s2}	Sumut	1570	2260.1	Belawan	163	74.27
				Labuhan Angin	105	
				Pangkalan Susu	400	
				Growth Sumatra	19	
				Growth Asia	20	
				PKS Rambutan	1.8	
				Harkat Sejahtera	10	
				Belawan	637	
				Belawan	90	
				Glugur	21	
				Paya Pasir	34	
				Titikuning	16	
				Rental Paya Pasir	115	
				Rental Belawan (AKE)	65	
				Rental Belawan MFO	120	
				Sibayak	10	
				Sipansipahoras	50	
				Lau Renun	80	
				Asahan	180	
				Inalum (Transfer)	90	
				Tersebar	5	
				Parlilitan	7.5	
				Silau	7.5	
				Hutaraja	5	
				Karai	8.3	
n_{s3}	Riau	526	468.1	Teluk Lembu	32	43.35
				Balai Pungut	34	
				Rental Teluk Lembu	122	
				Balai Pungut (ex Belawan)	40	
				Balai Pungut	100.1	
				Riau Power	26	
				Koto Panjang	114	
n_{s4}	Sumbar	487	642.4	Ombilin	133	30.1
				Teluk Sirih	200	
				Pauh Limo	49.5	
				Maninjau	67.8	
				Batang Agam	10.5	
				Singkarak	174.6	
				Selo Kencana	7	
n_{s5}	Jambi	272	284.9	Biomassa RSPL	10	95.0
				Batang Hari	56.6	
				Payo Selincah	93.6	
				Sei Gelam (CNG)	89.5	
				Sei Gelam	12	
				Tanjung Jabung	7.2	
				Payo Selincah	16	
n_{s6}	Bengkulu	123	253.3	Musi	209.5	0.36
				Tes	18.1	
				Tes extension	4.3	
				Lebong	11.5	
				Lahat	9.9	
n_{s7}	Sumsel	768	1530.2	Bukit Asam	233.1	51.22
				Simpang Belimbing	227	
				Rental PTBA	6	
				Banjarsari	220	
				Baturaja	20	
				Keramasan	24.8	
				Talang Dukuh	68.6	
				LM Borang	11	

(Contd...)

Table 5: (Continued)

Node	Subsystem	q_{di} (MW)	$\overline{q}_{si}$ (MW)	Power plant	(MW)	mc ($/MWH)
n_{s7}	Sumsel	768	1530.2	Bukit Asam	233.1	51.22
				Simpang Belimbing	227	
				Rental PTBA	6	
				Banjarsari	220	
				Baturaja	20	
				Keramasan	24.8	
				Talang Dukuh	68.6	
				LM Borang	11	
				Borang	67.2	
				Jakabaring	50.5	
				Rental Keramasan	45	
				Rental Jambi	29.7	
				Prabumulih	11.6	
				Sako	11.8	
				Musi Rawas	8	
				Borang	150	
				Indralaya	120.5	
				Gunung Megang	110	
				Musi II	19.4	
				Keramasan	74	
				Sungai Juaro	22	
n_{s8}	Lampung	851	579.5	Tarahan	178	33.38
				Sebalang	89	
				Gunung Sugih	14	
				Pelabuhan Tarahan	10	
				Tarahan	16	
				Tarahan	20.5	
				Teluk Betung	12.6	
				Tegineneng	18	
				Ulubelu	103.8	
				Besai	89.6	
				Batutegi	28	
	Total	4887	6282.7		6282.7	

Table 6: Transmission characteristic for Sumatra power system

Trans	From *i*		To *j*		X_{ij} (p.u)	T_l (MW)	Configuration
t_{s1}	1	Langsa	2	Pangkalan Brandan	0.06	591	2×78.27 km; AC3
t_{s2}	2	Kota Pinang	3	Bagan Batu	0.05	301.6	2×68 km; single Haw
t_{s3}	3	Koto Panjang	4	Payakumbuh	0.07	363.2	2×85 km; Duck
t_{s4}	4	Kiliranjao	5	Muarabungo	0.08	835	2×117 km; twin Zebra
t_{s5}	5	Bangko	7	Lubuk Linggau	0.13	835	2×195 km; twin Zebra
t_{s6}	7	Lubuk Linggau	6	Pekalongan	0.04	835	2×68 km; ACSR 2X340 mm2
t_{s7}	7	Baturaja	8	(Umpu - Kemuning)	0.10	446	1×98.37 km; AC3 (Kemuning)

Table 7: Shift factor matrix for Sumatra power system

1	0	0	0	0	0	0	0
1	1	0	0	0	0	0	0
1	1	1	0	0	0	0	0
1	1	1	1	0	0	0	0
1	1	1	1	1	0	0	0
0	0	0	0	0	1	0	0
1	1	1	1	1	1	1	0

Figure 10: Map of Sumatra power system

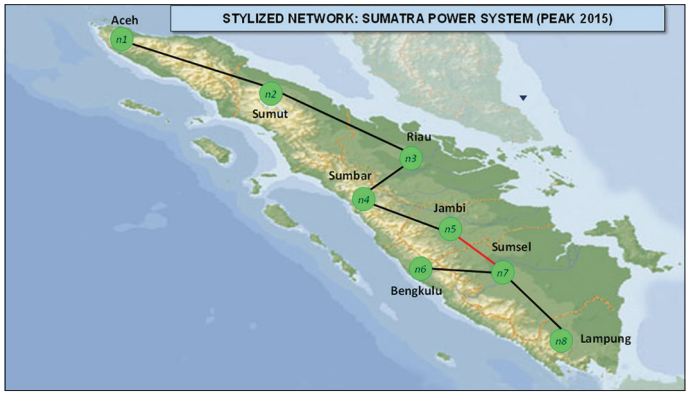

system suffers several power system constraints, i.e. transmission limit, small-signal stability, transient stability and subsystem interconnection. Small-signal stability is the system constraint related with network stability resulting from small disturbances that leads to power system oscillation. The power system is stable if the oscillation can be suppressed and system deviation remains low for a period of time. In contrast with small-signal stability, transient stability is caused by sudden and significant outages in the electrical network. The North Sumatra and Mid Sumatra subsystems were interconnected in 2007 through the 150 kV T/L

Table 8: Equilibrium of demand, generation, price and welfare for Sumatra power system

Node	Subsystem	q_{di} (MW)	q_{si} (MW)	p_i	PS	CS	TW
n_{s1}	Aceh	298.43	-	79.0	-	100,296	100,296
n_{s2}	Sumut	1,625.07	2,013.31	75.1	10,134	549,354	559,488
n_{s3}	Riau	542.41	468.1	77.6	11,375	182,673	194,049
n_{s4}	Sumbar	500.22	642.4	80.2	18,388	167,802	186,191
n_{s5}	Jambi	278.24	-	83.0	-	92,954	92,954
n_{s6}	Bengkulu	131.15	253.3	54.7	6,896	45,671	52,567
n_{s7}	Sumsel	818.85	1,145.16	54.7	3,278	285,142	288,420
n_{s8}	Lampung	907.41	579.5	54.7	7,732	315,995	323,727
	Total	5,101.8	5,101.8		57,803	1,739,887	1,797,690

Table 9: Power transfer for Sumatra nodal pricing

Trans	From node i	To node *j*	P_{ij} (DC) (MW)
t_{s1}	n_{s1}	n_{s2}	−298.4
t_{s2}	n_{s2}	n_{s3}	89.8
t_{s3}	n_{s3}	n_{s4}	15.5
t_{s4}	n_{s4}	n_{s5}	157.7
t_{s5}	n_{s5}	n_{s7}	−120.5
t_{s6}	n_{s6}	n_{s6}	122.2
t_{s7}	n_{s7}	n_{s8}	327.9

Bagan Batu - Kota Pinang. However, due to stability issue arising from interconnecting the two subsystems, the system remains separated. The line connecting these two subsystems is operated in normally-open condition. Hakam et al. (2011) for further explanation regarding transient stability and interconnection problems in the Sumatra power system.

Sumsel is dominated by Coal PP, i.e. Bukit Asam PP (233.1 MW), Simpang Belimbing PP (227 MW), Banjarsari PP (220 MW), Indralaya PP (120.5 MW), and Gunung Megang PP (110 MW). In contrast, generation technology in Jambi is dominated by gas and oil fuel-based PP, i.e., Batang Hari PP (56.6 MW), Payo Selincah PP (93.6 MW), and Sei Gelam CNG PP (89.5 MW). Sumsel provided a low fuel cost compared to Jambi and Lampung. The differences in fuel cost between Sumsel and Jambi as well as the energy deficit in the Middle Subsystem caused a significant load flow from South (node 7) to Mid Sumatra (node 6), especially on the peak load condition. The small signal stability limit caused a power transfer limitation to 230 MW.

Transmission constraints T_l reflects the cable thermal limit for a 150 kV overhead transmission lines. Small-signal stability constraint reduces the transfer limit of t_{s5} which connects the South and Mid Sumatra subsystems to 230 MW. Interconnection constraints between the North and Mid Sumatra subsystems limit the cable limit of t_{s2} to 90 MW which reflects the actual demand in the nearest substation. The thermal constraint in t_{s7}, and stability constraints in t_{s5}, are normally binding and have an impact on the prices since the Sumsel subsystem transports energy at lower price compared to the importer subsystems (Lampung and Jambi).

Table 9 above shows the DC power transfer flow for the Sumatra power system. The arc of load flow is influenced by the power injection of each node (q_{si}=q_{di}). The negative sign in t_{s1} and t_{s5} shows that load flow has an opposite direction to the anchor points, i.e. load flow for transmission t_{s1} is from Pangkalan Brandan (Sumut subsystem) to Langsa (Aceh subsystem) while load flow for transmission t_{s5} is from Lubuk Linggau (Sumsel subsystem)

Figure 11: Load flow realisation of Sumatra power system (P3BS, 2016a)

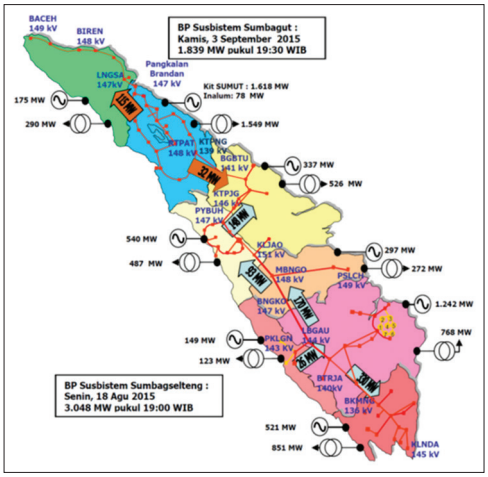

to Bangko (Jambi subsystem). Power transfer from Sumsel to Lampung is 327 MW, while the cable limit of t_{s7} is 446.3 MW. Thus, the transmission t_{s7} does not meet the contingency N-1 criteria (collapse in one overhead cable will cause the collapse of transmission lines). Note that power transfer from Sumsel to Jambi (120.5 MW) is below the limit of small signal stability constraint (230 MW).

Thermal constraint in t_{s5} is bound to the equilibrium due to Lampung as a deficit subsystem. Thus, Lampung needs electricity imported from the connected subsystem (South Sumatra). In contrast, Jambi is a surplus region where the Jambi power plants can adequately produce electricity for Jambi's LSE. However, Jambi has a higher fuel cost and electricity price compared to South Sumatra. Instead of producing its own electricity, Jambi imports all required electrical energy from South Sumatra. It can be seen from Table 9 that South Sumatra has a surplus electricity energy of 326 MW to transfer into the Lampung and Jambi subsystems.

The simulation result in Case 1 is similar with the power system realisation as in Figure 11. As mentioned earlier in Chapter 3, this research assumes the full available capacity of Hydro PP. In addition, this study ignores the TOP (Take or Pay) contract between IPP and primary energy producers with PLN. Therefore, as can be compared in Table 9 and Figure 11, there are differences in power transfer, especially for the transmission lines connecting the Sumbar and Bengkulu nodes[3].

3 Sumbar and Bengkulu are abundant with hydro resources compared to other nodes.

The stylised models in this research do not fully accurately represent the real power system at the detailed level of a low voltage power substation. However, the modelling was based on the actual network topology of a 150-kV power network by using a bottom-up approach. In the Sumatra system, cable lines connect two power substation (SS) at the end of each node, i.e., transmission line t_{s1} is connecting the 150 kV Langsa SS at n_{s1} Aceh with the 150 kV Pangkalan Brandan SS at n_{s2} Sumut. Thus, the model will response in a similar way compared to the actual power system in responding to any changes in generation and demand.

5. CONCLUSIONS

Based on the simulation in the chapter 4, we found that the price (p_i) in each nodal could be different if there is a network constraint in the electricity mesh network. In a non-constraints network, the nodal price is equivalent for each node although there is a deviation of true marginal cost between generating firm. Transmission and generation system constraints affect the equilibrium nodal prices. The welfare was reduced when the transmission has limited transfer capability.

This research presents a stylised economic model of the Indonesia electricity market to calculate nodal pricing of Indonesia's power system with engineering constraints. This study is the first study that analyses LMP using perfect competition optimisation in the Indonesia electricity market which contributes to the current academic literature. This model uses actual power system data from 2015 that was acquired from PLN, an Indonesia state-owned electricity company. This nodal pricing model is based on a simplified DC load flow by applying the PTDF to the equation and comparing it with the actual power transfer realisation. The electricity stakeholder in Indonesia could apply this nodal pricing regime rather than uniform price regime to increase the society welfare. By using this model, PLN could mitigate the risk of power generation investment by invest in power generation efficiently according to the economic signals from nodal pricing modelling.

6. ACKNOWLEDGMENT

We acknowledged the support from Indonesia Endowment Fund for Education (LPDP).

REFERENCES

ESDM. (2015), Ministry of Energy and Mineral Resources Regulation No. 31 Year 2014 Regarding Electric Energy Tariff Provided by PLN. Indonesia.

Faizal, R., Muhammad, N., Ricky, F., Stephan, P. (2015), Sumatra-Java HVDC Transmission System Modelling And System Impact Analysis. Conference: 2015 IEEE Eindhoven PowerTech.

Green, R. (2007), Nodal pricing of electricity: How much does it cost to get it wrong? Journal of Regulatory Economics, 31(2), 125-149.

Hagspiel, S., Jagemann, C., Lindenberger, D., Brown, T., Cherevatskiy, S., Troster, E. (2014), Cost-optimal power system extension under flow-based market coupling. Energy, 66, 654-666.

Hakam, D.F., Ayodele, A. (2018), Gas monetisation intricacies: Evidence from Indonesia. International Journal of Energy Economics and Policy, 8(2), 174-181.

Hakam, D.F., Luqman, A., Taufiq, F. (2012), Sustainable Energy Production In Sumatra Power System. Bali, Indonesia: In IEEE Conference on Power Engineering and Renewable Energy 2012, J2.

Hakam, D.F., Rizki, W., Eko, Y.P. (2011), Switching Study for 275 kV Padang Sidempuan-Payakumbuh Transmission Line. Bandung, Indonesia: 2011 International Conference on Electrical Engineering and Informatics. pE10-3.

Hogan, W., Juan, R., Ingo, V. (2010), Toward a combined merchant-regulatory mechanism for electricity transmission expansion. Journal of Regulatory Economics, 38(2), 113-143.

Leuthold, F.U., Hannes, W., Christian, H. (2012), A large-scale spatial optimization model of the European electricity market. Networks and Spatial Economics, 12(1), 75-107.

Macatangay, R. (1998), Space-time prices of wholesale electricity in England and Wales. Utilities Policy, 7(3), 163-188.

P3BS. (2016a), Operation Evaluation Year 2015: Sumatra Power System. Pekanbaru, Indonesia.

P3BS. (2016b), Operation Planning Year 2016: Sumatra Power System. Pekanbaru, Indonesia.

PLN. (2015), Rencana Umum Penyediaan Tenaga Listrik (National Electricity Supply Business Plan) PT PLN (Persero) 2015-2024. Jakarta, Indonesia. Available from: http://www.pln.co.id/dataweb/RUPTL/RUPTL PLN 2015-2024.pdf.

Schweppe, F., Michael, C., Richard, T., Roger, B. (1988), Spot Pricing of Electricity. The Kluwer International Series in Engineering and Computer Science. 1st ed. Massachusetts: Kluwer Academic Publishers.

Wartana, I.M., Singh, J.G., Werakorn, O., Ni, P.A. (2012), Optimal Placement of a Series FACTS Controller in Java-Bali 24-Bus Indonesian System for Maximizing System Loadability by Evolutionary Optimization Technique. Proceedings - 3rd International Conference on Intelligent Systems Modelling and Simulation, ISMS. p516-521.